Discovery of 21 CLQs in the northern sky based on optical/MIR variability

Xue-Bing WU
(DoA & KIAA, Peking Univ., China)

Collaborators: Qian Yang (UIUC), Xiaohui Fan (Arizona), Yue Shen (UIUC)

Presented in “Quasars in Crisis” ,
Royal Observatory Edinburgh, UK; 2019/08/06-09

Content

1. Introduction
2. New discoveries of CLQs
3. Challenges to theoretical models
4. Summary

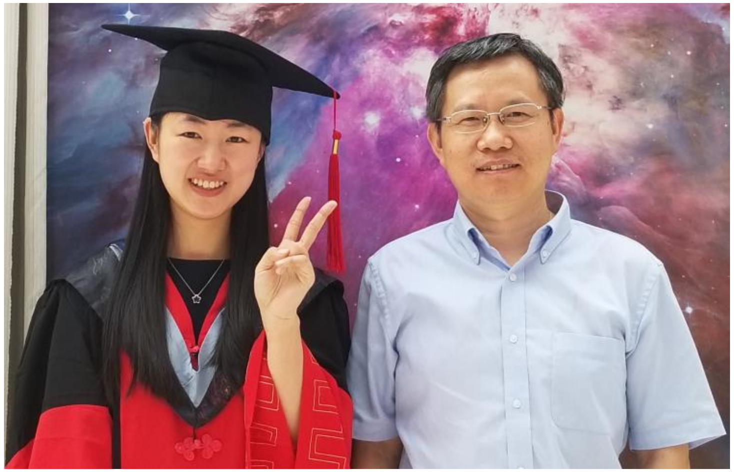

(Yang Q., Wu X.-B., Fan X., et al. 2018, ApJ, 862, 109)

1. Introduction

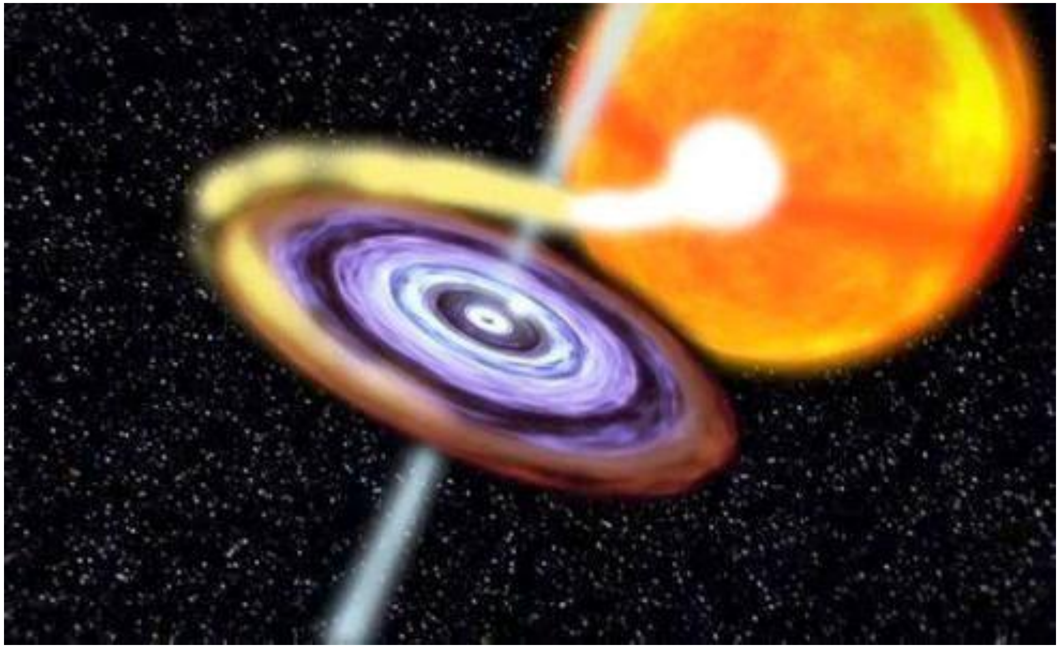

Stellar mass BHs（~10 solar masses）in X-ray binaries

Supermassive BHs（10^6-10^{10} solar masses）in quasars / the center of galaxies

X-ray variability in BH XRB-> different states

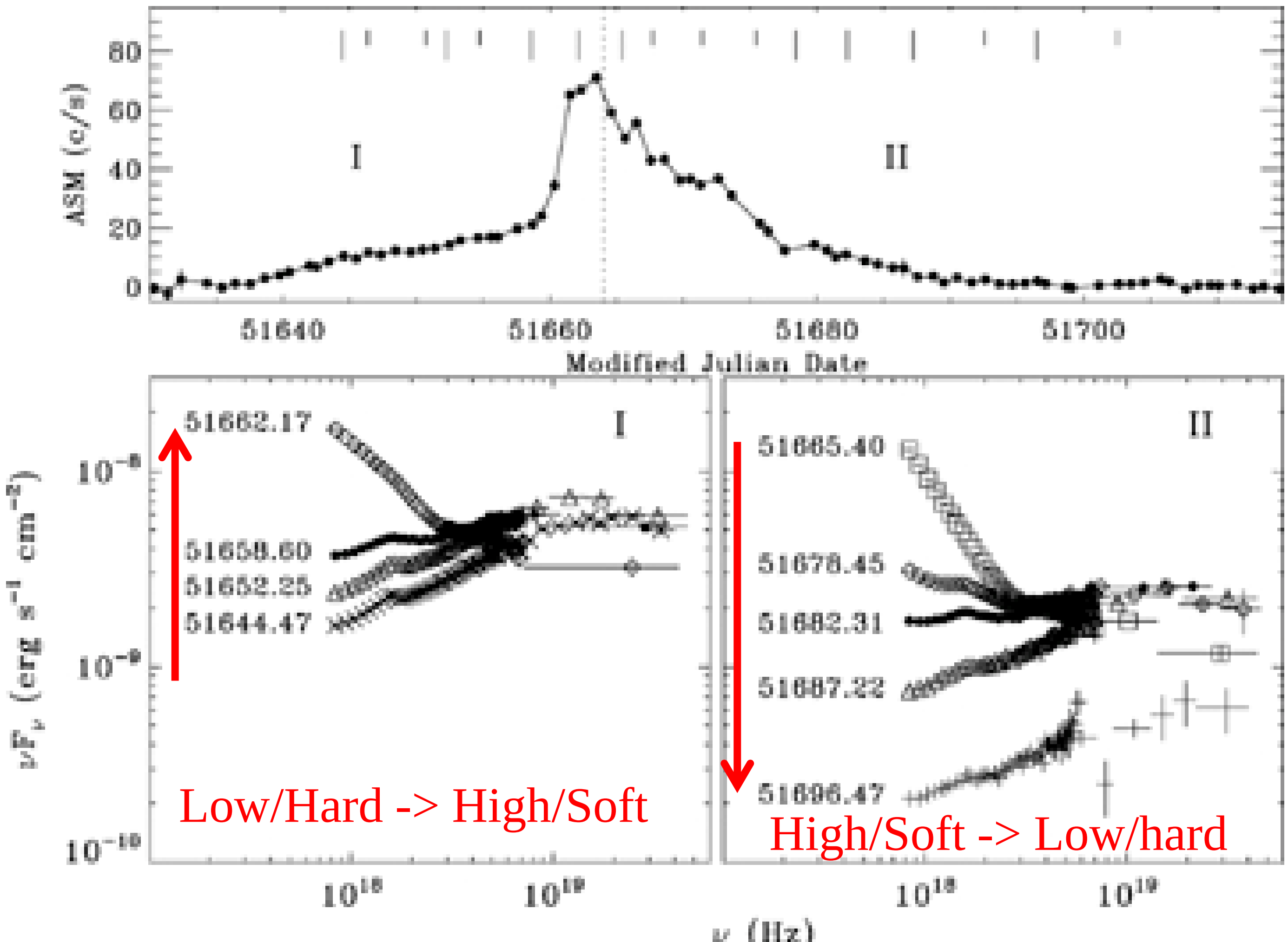

Timescale: days to weeks

ASM/RXTE light curve of XTE J1550−564 in 2000 (Xue, Wu & Cui, 2008, MNRAS, 384, 440)

Accretion rate change and timescale

- Variation of soft component in BH X-ray binaries

GRS 1915+105

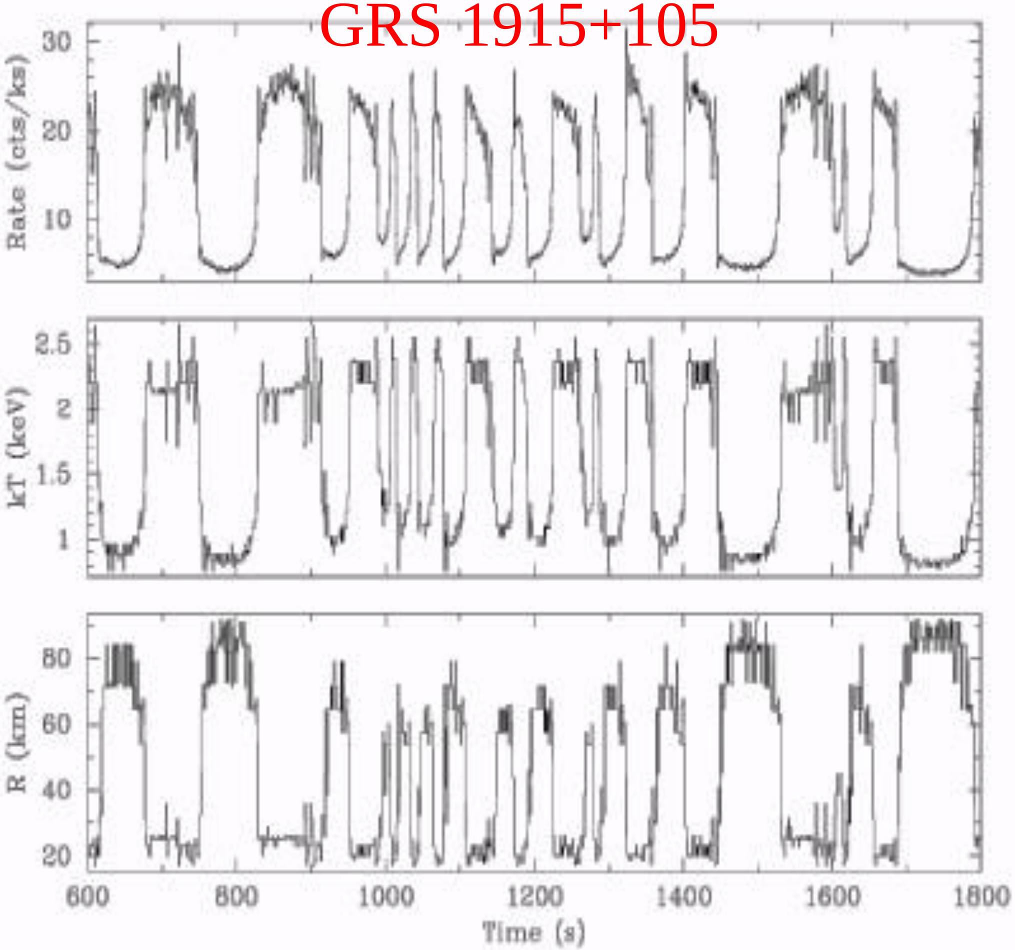

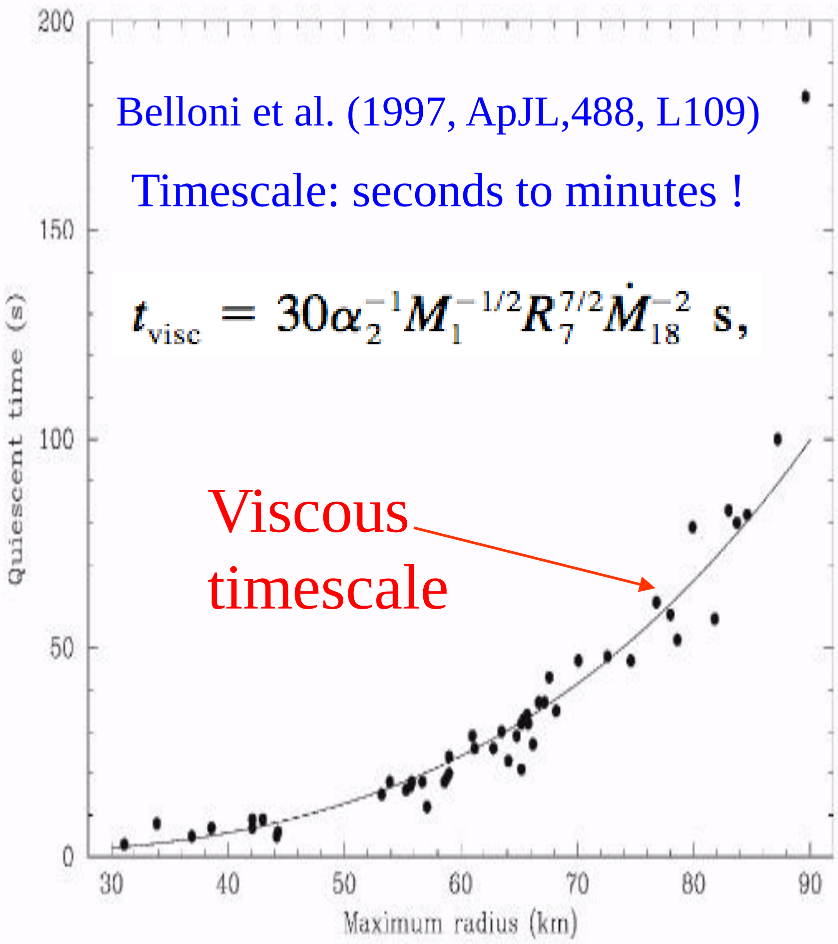

Belloni et al. (1997, ApJL,488, L109)

Timescale: seconds to minutes !

$$t_{\rm visc} = 30\alpha_2^{-1} M_1^{-1/2} R_7^{7/2} \dot{M}_{18}^{-2} \ {\rm s},$$

Viscous timescale

Some AGNs show disappearance and/or re-appearance of broad emission lines in optical spectra within several tens of years ! -> **Changing-look AGN**

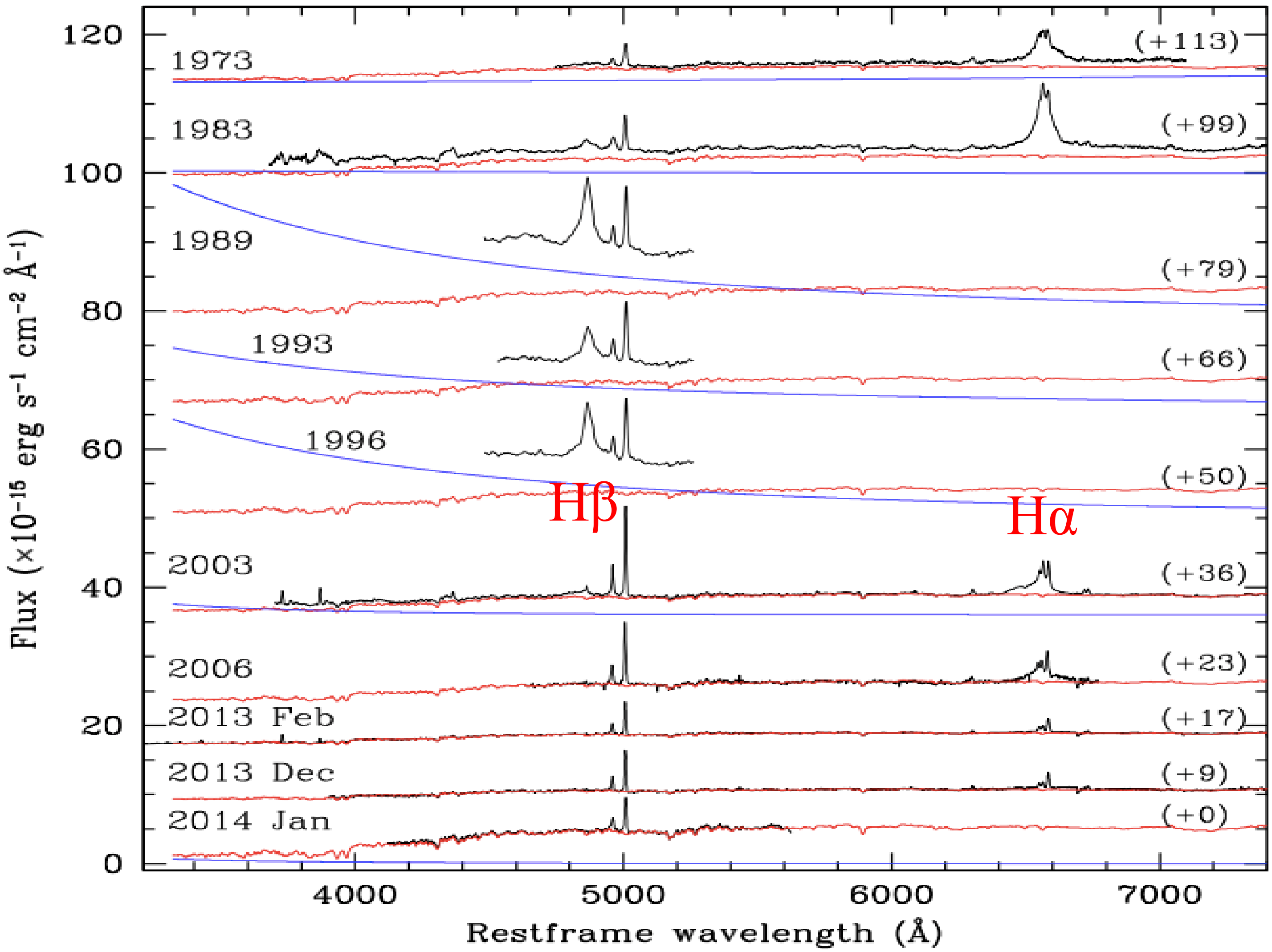

Seyfert G., Mrk 590

Denney et al. 2014, ApJ

Chandra X-ray Spectra of Mrk 590

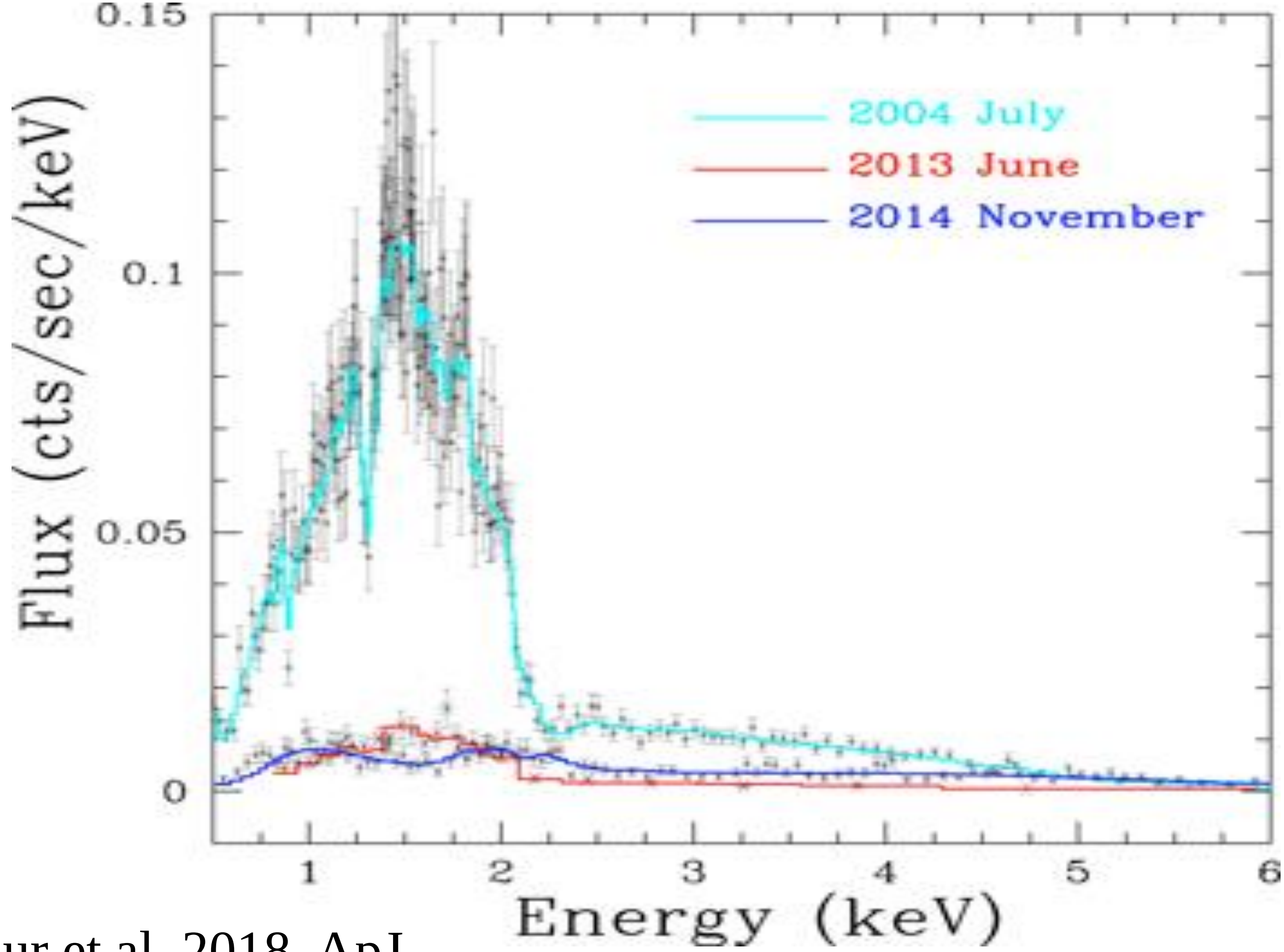

Mathur et al. 2018, ApJ

Gezari et al. 2017

Turn-on

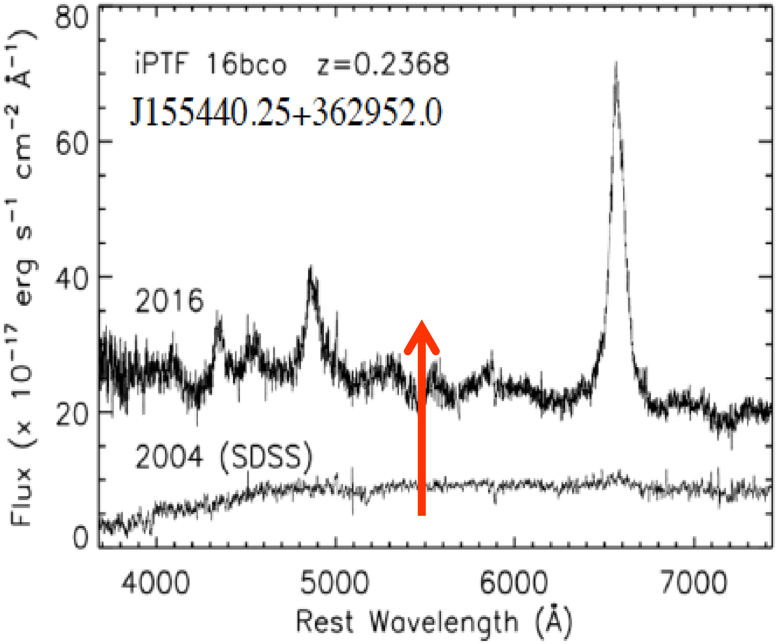

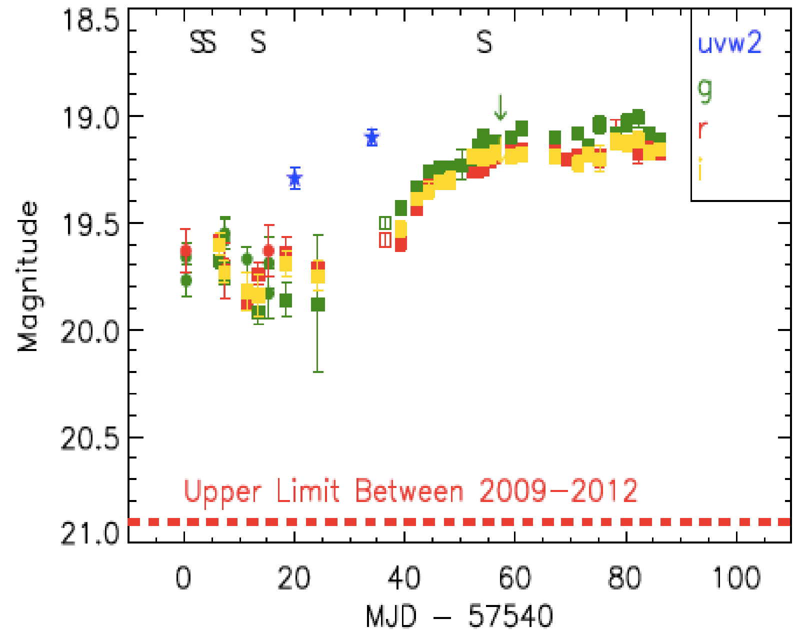

Runnoe et al. 2016

Turn-off

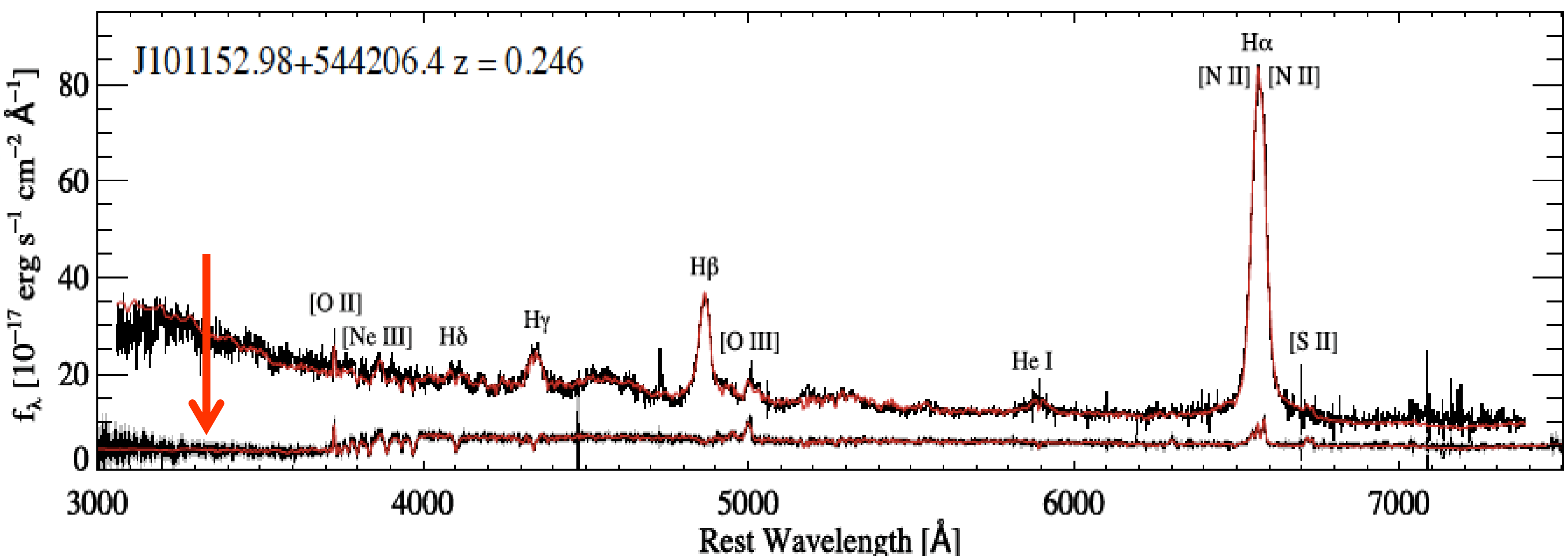

Previous discoveries

- Mrk 1018: Type 1.9 to Type 1, and back to Type 1.9 after 30 years (Cohen et al. 1986; McElroy et al. 2016)
- Mrk 590: Type 1.5 to Type 1 and back to Type 1.9-2 (Denney et al. 2014)
- NGC 2617: Seyfert 1.8 galaxy (Moran et al. 1996), changed to a Seyfert 1 (Shappee et al. 2014).
- LaMassa et al. (2015): the first CL quasar, J0159+0033, changed from Type 1 to Type 1.9.
- Runco et al. (2016): broad Hβ line virtually disappears in 3/102 local Seyfert galaxies
- Runnoe et al. (2016): a CL quasar, J1011+5442, "turning-off" within a rest-frame time of ~ 500 days.
- A quasar, J1554+3629, turned on in a timescale shorter than 1 year (Gezari et al. 2017).
- Systematic archival searches in SDSS with repeat spectroscopy: 13 CLQs (Ruan et al. 2016; MacLeod et al. 2016) and more (MacLeod et al. 2019)
- Wang J. et al. (2018): SDSS J141324.27+530527.0, a New "Changing-look" Quasar with a "Turn-on" Transition (see poster of Dawei Xu)

Mid-infrared Variability of Changing-look AGNs (Sheng, Wang, Jiang et al. 2017, ApJL)

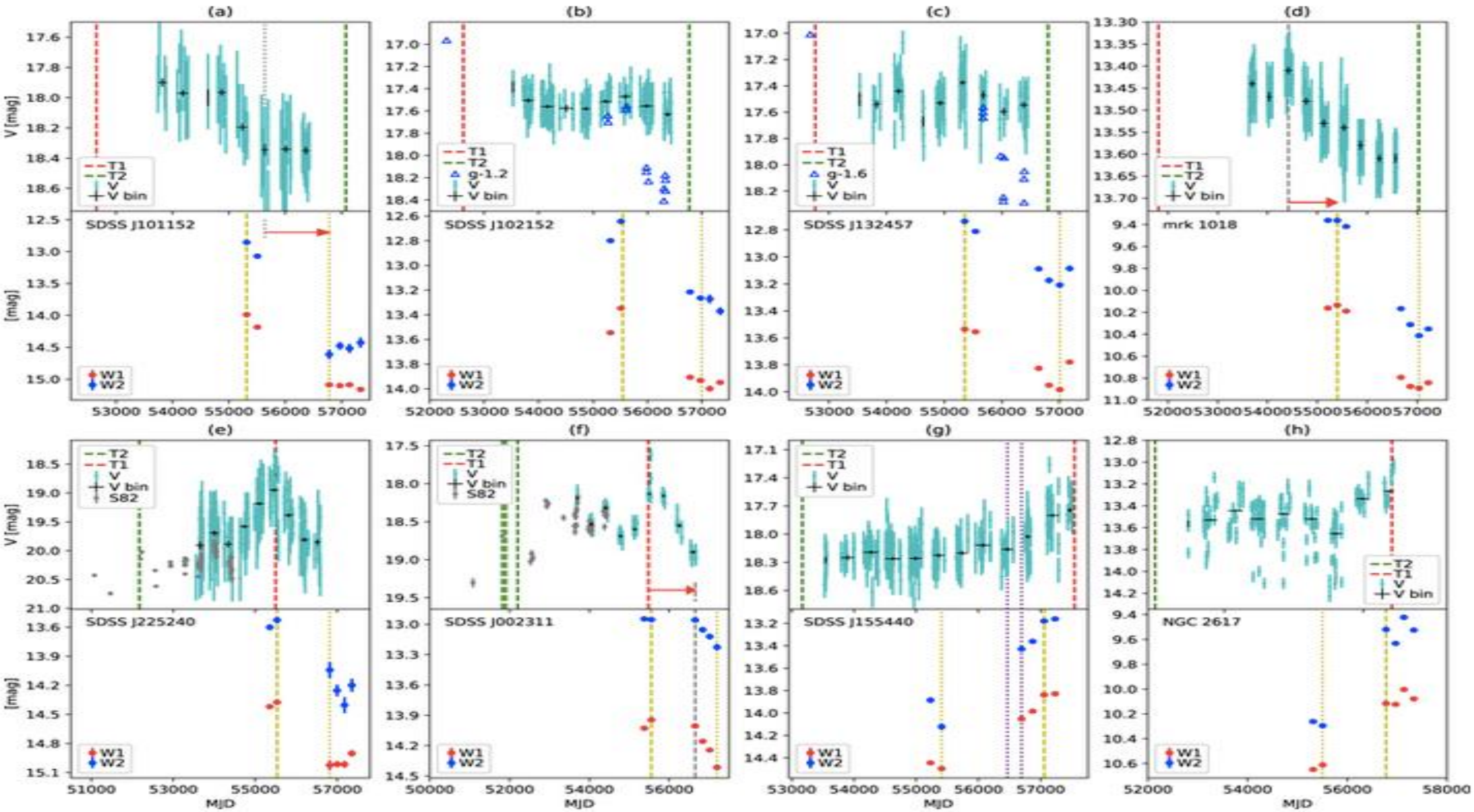

The mid-infrared light curves of 10 objects echo the variability in the optical band with a time lag (years) expected for dust reprocessing.

2. New discoveries of CLQs

(Yang, Wu, Fan, et al. 2018, ApJ, 862, 109)

- Telescopes we used for spectroscopy
  - LAMOST: Chinese 4m spectroscopic survey telescope
    - 4000 fibers, 20 square degrees
    - Obtained spectra of 10million bright stars and 200k galaxies/quasars
  - 2.4m Lijiang telescope and 2.16m Xinglong telescope
  - Palomar 5m Hale telescope

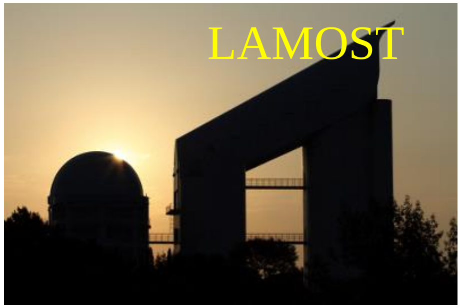

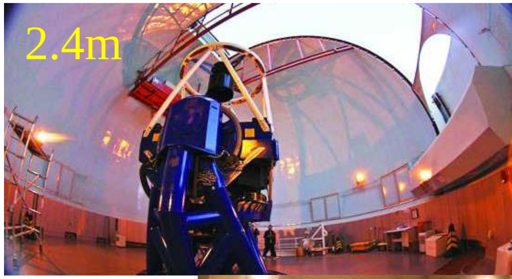

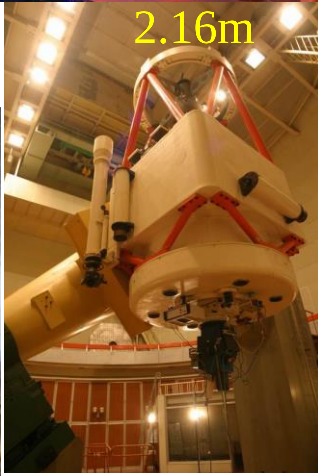

- Multi-epoch spectra
  - SDSS spectral archive => 9 CLQs (4 known)
  - SDSS-LAMOST spectral archive => 10 CLQs

- Photometric variability + New spectroscopy => 7 CLQs (1 known)
  - Galaxies brightened
  - Quasars dimmed
    - Photometric data used:
    - \- SDSS
    - \- Pan-STARRS
    - \- DESI imaging
    - \- WISE
    - \- Catalina Real-time Transient Survey (CRTS)
    - \- Palomar Transient Factory (PTF)

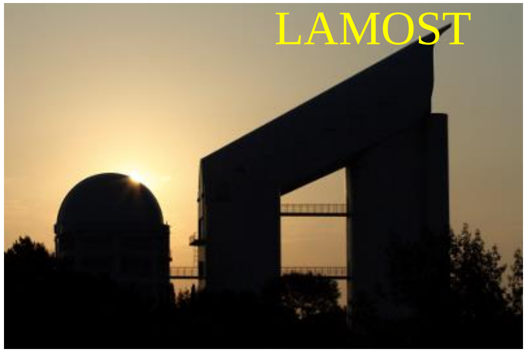

Extensive searches in repeat spectra from SDSS & LAMOST

Table 1
CL AGNs Selection from SDSS Repeat Spectra

Note	Selection	Number
Spectra in SDSS DR14	All	4,851,200 spectra
Spectra with good quality	*zWarning* = 0 or 16	4,196,290 spectra
Objects with repeat spectra	$2''$ coordinates cross-match	350,609 objects
Galaxies with repeat spectra	classified as "GALAXY" at one epoch	175,575 objects
Classification changed between QSO and Galaxy	classified as "QSO" at another epoch	2,023 objects
Visual check	appearing or disappearing broad Hβ	9 (4 known) CL AGNs

Table 2
CL AGNs Selection from SDSS and LAMOST Repeat Spectra

Note	Selection	Number
Spectra with good quality	*zWarning* = 0 or 16	4,196,290 spectra
SDSS QSO/Galaxy	classified as "GALAXY" or "QSO"	3,223,478 spectra
Repeatedly observed by LAMOST	$2''$ cross-match with LAMOST	155,220 objects
Possible variable Balmer lines	program to automatically check emission-line variation	8,181 objects
Visual check	appearing or disappearing broad Hβ	10 CL AGNs

Extensive searches in opt/mid-IR variability…

Table 3
Turn-on CL AGN Candidate Selection Based on Imaging Data

Turn on

Note	Selection	Number
Spectra in SDSS DR14	all	4,851,200 spectra
WISE single-epoch detected	2″ cross-match with the *WISE* single-epoch data	4,196,290 spectra
Galaxies with good spectra	class="GALAXY" and ($zWarning$ = 0 or 16)	2,494,319 spectra
WISE brighten and redder	$\Delta W1 < -0.2$ and $\Delta(W1 - W2) > 0.1$	28,395 objects
Optical brighten	$\Delta g < 0$ and $g < 19$	2147 objects
Redshift	$z > 0.1$	660 objects
Visual check light curves	obvious brighten trend (CRTS/PTF)	59 objects
Observed	···	17 objects
Confirmed	···	6 (1 known) CL AGNs

Table 4
Turn-off CL AGN Candidate Selection Based on Imaging Data

Turn off

Note	Selection	Number
SDSS QSO in DR7 and DR12	All	346,464 objects
WISE single-epoch detected	2″ cross-match with the *WISE* single-epoch photometry	326,124 objects
WISE dim and bluer	$\Delta W1 > 0.2$ and $\Delta(W1 - W2) < -0.1$	6,847 objects
Optical dim	$\Delta g > 1$	232 objects
Observed	···	1 objects
Confirmed	···	1 CL AGN c

New CLQs: turn on

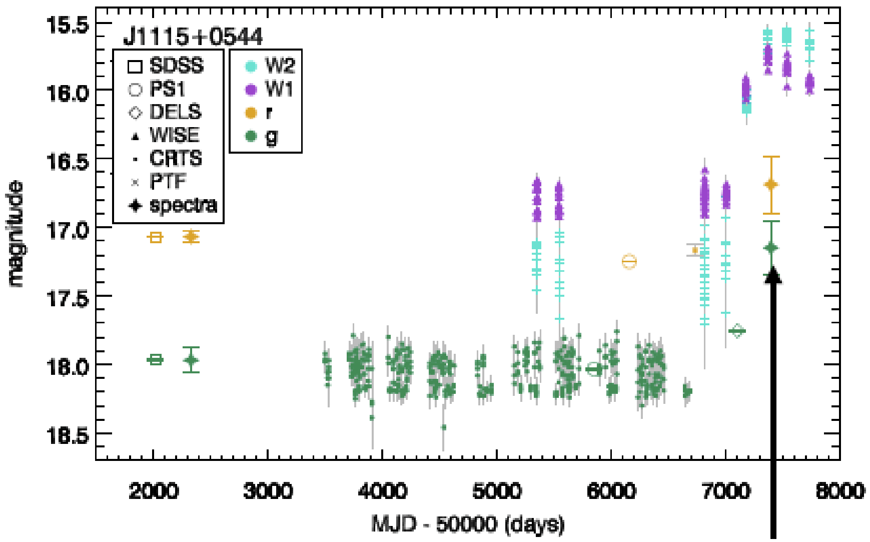

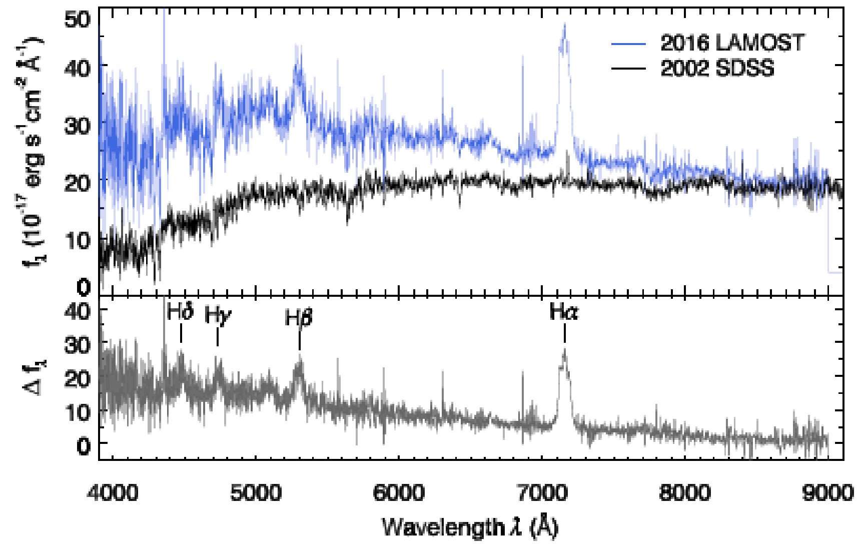

~1 mag brightened in optical and infrared within 0.9 yr

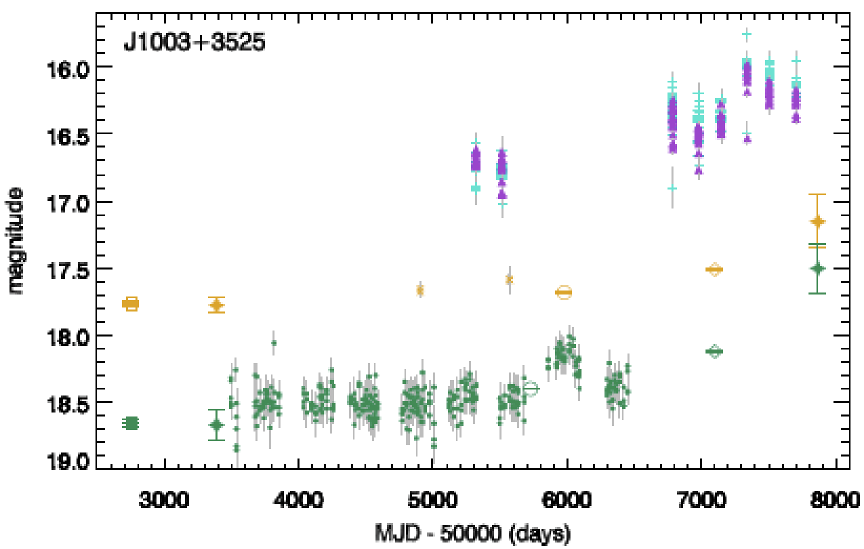

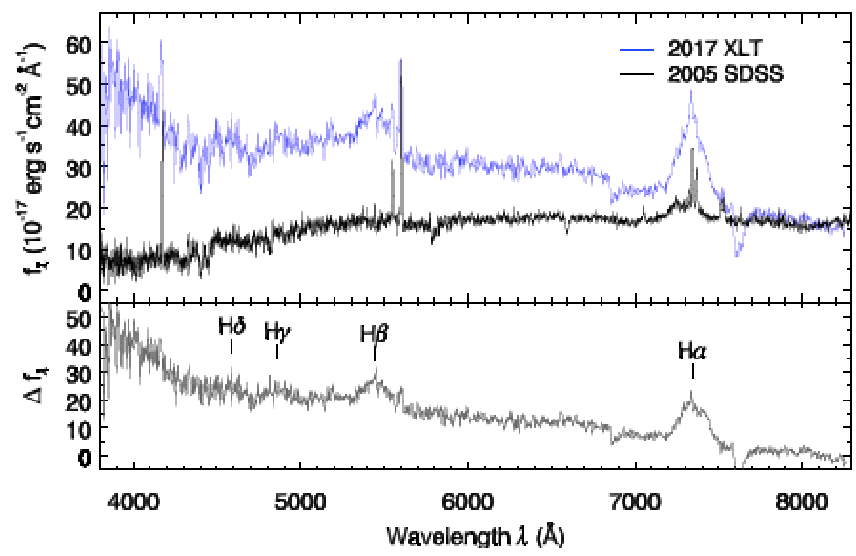

New CLQs: turn off

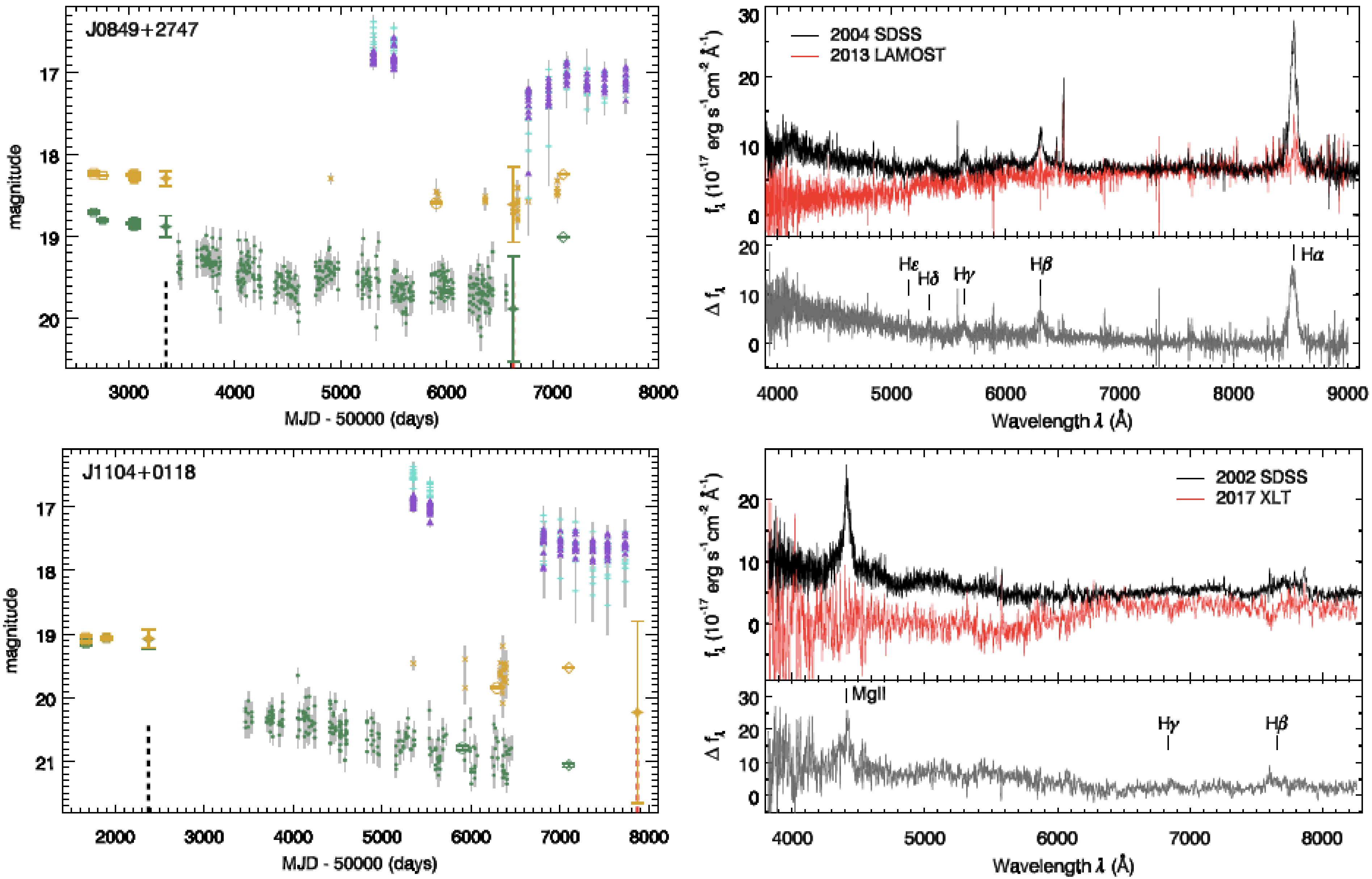

Turn on: 15 (+1); Turn off: 6 (+4)

Table 5
CL AGNs

Name	R.A.	Decl.	Redshift	Transition	Epoch	Instrument2	References
J0831+3646	08:31:32.25	+36:46:17.2	0.19501	Turn-on	[52312, 57367]	LAMOST	This work
J0849+2747	08:49:57.78	+27:47:28.9	0.29854	Turn-off	[53350, 56628]	LAMOST	This work
J0909+4747	09:09:32.02	+47:47:30.6	0.11694	Turn-on	[52620, 57745]	LAMOST	This work
J0937+2602	09:37:30.32	+26:02:32.1	0.16219	Turn-on	[54524, 57369]	LAMOST	This work
J1003+3525	10:03:23.47	+35:25:03.8	0.11886	Turn-on	[53389, 57867]	XLT	This work
J1104+0118	11:04:55.17	+01:18:56.6	0.57514	Turn-off	[52374, 57867]	XLT	This work
J1104+6343	11:04:23.21	+63:43:05.3	0.16427	Turn-off	[52370, 54498]	SDSS	This work
J1110−0003	11:10:25.44	−00:03:34.0	0.21922	Turn-on	[51984, 57864]	XLT	This work
J1115+0544	11:15:36.57	+05:44:49.7	0.08995	Turn-on	[52326, 57393]	LAMOST	This work
J1118+3203	11:18:29.64	+32:03:59.9	0.3651	Turn-off	[53431, 56367]	BOSS	This work
J1132+0357	11:32:29.14	+03:57:29.0	0.09089	Turn-on	[52642, 57392]	LAMOST	This work
J1150+3632	11:50:39.32	+36:32:58.4	0.34004	Turn-off	[53436, 57422]	BOSS	This work
J1152+3209	11:52:27.48	+32:09:59.4	0.37432	Turn-off	[53446, 57844]	LAMOST	This work
J1259+5515	12:59:16.74	+55:15:07.2	0.19865	Turn-on	[52707, 57863]	XLT/DBSP	This work
J1319+6753	13:19:30.75	+67:53:55.4	0.16643	Turn-on	[51988, 57867]	XLT	This work
J1358+4934	13:58:55.82	+49:34:14.1	0.11592	Turn-on	[53438, 54553]	SDSS	This work
J1447+2833	14:47:54.23	+28:33:24.1	0.16344	Turn-on	[53764, 57071]	LAMOST	This work
J1533+0110	15:33:55.99	+01:10:29.7	0.14268	Turn-on	[51989, 54561]	SDSS	This work
J1545+2511	15:45:29.64	+25:11:27.9	0.11696	Turn-on	[53846, 57891]	LAMOST	This work
J1550+4139	15:50:17.24	+41:39:02.2	0.22014	Turn-on	[52468, 57864]	XLT	This work
J1552+2737	15:52:58.30	+27:37:28.4	0.08648	Turn-on	[53498, 56722]	LAMOST	This work
J0126−0839	01:26:48.08	−08:39:48.0	0.19791	Turn-off	[52163, 54465]	SDSS	Ruan et al. (2016)
J0159+0033	01:59:57.64	+00:33:10.5	0.31204	Turn-off	[51871, 55201]	BOSS	LaMassa et al. (2015)
J1011+5442	10:11:52.98	+54:42:06.4	0.24639	Turn-off	[52652, 57073]	BOSS	Runnoe et al. (2016)
J1554+3629	15:54:40.26	+36:29:51.9	0.23683	Turn-on	[53172, 57862]	XLT	Gezari et al. (2017)
J2336+0017	23:36:02.98	+00:17:28.7	0.24283	Turn-off	[52199, 55449]	BOSS	Ruan et al. (2016)

Almost double the number of changing-look AGNs,;The upper limit of type transition timescale ranges from 0.9 to 12.6 years in the rest-frame.

Spectral Changes(2->1;1->2)

Table 6
Spectral Type Transition of CL AGNs

Name	Redshift	λL_{5100} (10^{42} erg s^{-1})	S/N$_1$	S/N$_2$	$L_{\mathrm{H}\beta,1}$ (10^{41} erg s^{-1})	$L_{\mathrm{H}\beta,2}$ (10^{41} erg s^{-1})	$L_{\mathrm{H}\alpha,1}$ (10^{41} erg s^{-1})	$L_{\mathrm{H}\alpha,2}$ (10^{41} erg s^{-1})	S/N$_{\mathrm{H}\beta_1}$	S/N$_{\mathrm{H}\beta_2}$	S/N$_{\mathrm{H}\alpha_1}$	S/N$_{\mathrm{H}\alpha_2}$	E1	E2	Type
J0831+3646	0.19501	18.23 ± 0.24	12.3	10.9	-4.05 ± 0.33	2.85 ± 0.39	3.60 ± 1.00	10.19 ± 0.42	−12.1	7.3	3.6	24.2	2	1	on
J0849+2747	0.29854	63.42 ± 1.48	9.3	2.7	8.56 ± 0.39	-2.81 ± 2.03	22.76 ± 1.95	2.49 ± 0.97	22.2	−1.4	11.7	2.6	1	2	off
J0909+4747	0.11694	6.97 ± 0.20	11.0	8.5	-1.88 ± 0.13	1.32 ± 0.18	1.48 ± 0.13	7.39 ± 0.13	−14.9	7.5	11.8	57.1	1.9	1	on
J0937+2602	0.16219	6.85 ± 0.32	20.9	7.1	-1.71 ± 0.13	1.75 ± 0.20	3.66 ± 0.24	11.93 ± 2.04	−12.8	8.6	15.4	5.9	1.9	1	on
J1003+3525	0.11886	45.77 ± 1.64	15.6	6.9	-1.40 ± 0.12	10.30 ± 1.02	2.34 ± 0.57	12.58 ± 0.63	−11.7	10.1	4.1	19.9	2	1	on
J1104+0118	0.57514	302.41 ± 6.30	7.0	0.7	79.89 ± 5.19	-43.38 ± 13.61	...	...	15.4	−3.2	...	...	1	2	off
J1104+6343	0.16427	4.46 ± 0.49	6.0	6.1	1.14 ± 0.14	0.33 ± 0.11	4.90 ± 0.16	0.79 ± 0.13	7.9	3.0	31.6	6.2	1	1.8	off
J1110−0003	0.21922	48.61 ± 1.34	8.0	6.1	0.27 ± 0.10	6.70 ± 0.92	1.78 ± 0.71	11.98 ± 1.01	2.8	7.3	2.5	11.9	2	1	on
J1115+0544	0.08995	17.27 ± 0.27	18.9	8.7	-1.23 ± 0.07	2.46 ± 0.18	0.05 ± 0.07	7.92 ± 1.11	−18.4	14.0	0.7	7.2	2	1	on
J1118+3203	0.3651	56.48 ± 2.29	4.9	4.9	11.76 ± 1.11	2.90 ± 0.51	...	10.31 ± 0.57	10.6	5.7	...	18.0	1	1	off*
J1132+0357	0.09089	16.26 ± 0.38	17.3	7.4	-3.23 ± 0.08	4.74 ± 0.40	0.78 ± 0.05	2.40 ± 0.17	−40.2	11.8	15.9	14.1	1.9	1	on
J1150+3632	0.34004	39.01 ± 2.28	4.9	5.2	5.02 ± 0.53	-3.29 ± 0.49	22.24 ± 1.25	3.18 ± 0.40	9.4	−6.7	17.8	7.9	1	1.9	off
J1152+3209	0.37432	138.05 ± 2.68	11.9	3.7	38.31 ± 1.16	10.53 ± 1.29	...	...	33.0	8.2	...	...	1	1	off*
J1259+5515	0.19865	17.95 ± 0.91	7.4	3.5	0.02 ± 0.24	5.53 ± 0.82	4.30 ± 0.38	9.21 ± 3.88	0.1	6.8	11.4	2.4	1.9	1	on
J1319+6753	0.16643	30.90 ± 1.46	12.1	7.3	0.36 ± 0.33	7.96 ± 1.16	2.37 ± 0.27	5.90 ± 4.43	1.1	6.8	8.6	1.3	1.9	1	on
J1358+4934	0.11592	5.50 ± 0.19	7.8	13.1	0.36 ± 0.09	0.96 ± 0.10	0.74 ± 0.06	1.98 ± 0.10	3.8	9.2	13.4	19.0	1.9	1	on
J1447+2833	0.16344	66.68 ± 0.97	7.8	13.1	-1.16 ± 0.29	2.49 ± 0.24	2.27 ± 0.19	11.63 ± 0.25	−3.9	10.6	12.2	47.2	1.9	1	on
J1533+0110	0.14268	<1.00	14.2	13.4	-3.98 ± 0.17	0.54 ± 0.12	1.00 ± 0.15	3.97 ± 0.29	−23.6	4.4	6.9	13.7	1.9	1.5	on
J1545+2511	0.11696	6.81 ± 0.06	19.6	17.1	-2.16 ± 0.15	0.71 ± 0.11	1.69 ± 0.12	5.90 ± 0.14	−14.4	6.7	14.4	41.3	1.9	1	on
J1550+4139	0.22014	28.26 ± 1.30	11.6	8.1	-4.41 ± 0.47	15.71 ± 1.48	2.47 ± 0.40	14.01 ± 0.89	−9.5	10.6	6.2	15.8	1.9	1	on
J1552+2737	0.08648	<1.00	12.3	7.8	-3.67 ± 0.05	-1.34 ± 0.10	0.38 ± 0.04	2.70 ± 0.05	−69.2	−13.9	9.8	59.1	1.9	1.9	on*

Note. λL_{5100} is the continuum luminosity at 5100 Å in the bright epoch spectrum. J1533+0110 and J1552+2737 are too red to fit a power-law continuum, with a upper limit of 1.00×10^{42} erg s^{-1}. S/N$_1$ and S/N$_2$ are the median S/N pixel^{-1} of the former and recent epoch spectra, respectively. $L_{\mathrm{H}\beta,1}$, ($L_{\mathrm{H}\alpha,1}$) and $L_{\mathrm{H}\beta,2}$ ($L_{\mathrm{H}\alpha,2}$) are the luminosities of the broad Hβ (Hα) component in the former and recent epoch spectra. The negative luminosity means that there is absorption instead of emission lines. There is no Hα data when Hα moves out of the range of the spectrum. S/N$_{\mathrm{H}\beta_1}$ (S/N$_{\mathrm{H}\alpha_1}$) and S/N$_{\mathrm{H}\beta_2}$ (S/N$_{\mathrm{H}\alpha_2}$) are the S/Ns of broad Hβ (Hα) components in the former and recent epoch spectra. E1 and E2 describe the spectral types of the former and recent epoch spectra. Type describes the transition type.

Optical/Mid-IR Color changes

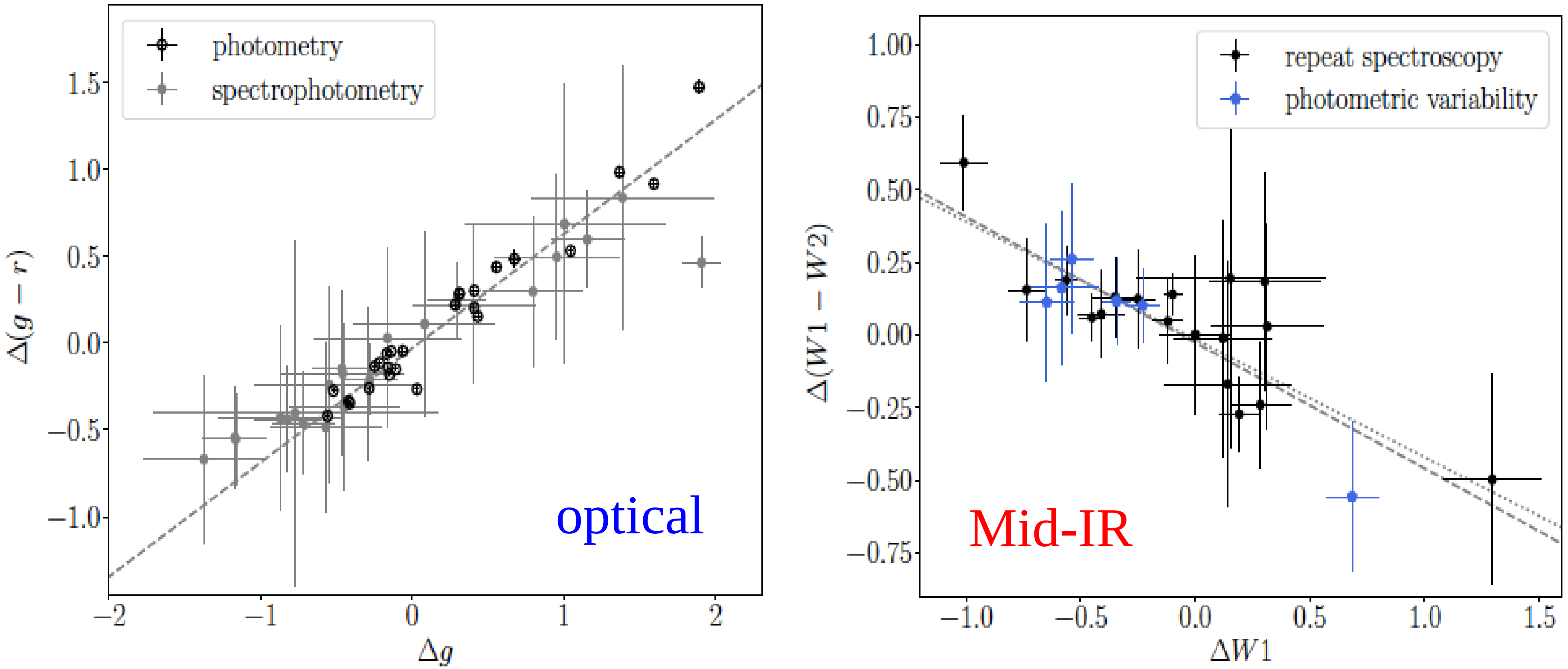

- A blueer-when-brighter chromatism is confirmed in optical band.
- The mid-infrared W1 − W2 color is redder when brighter.

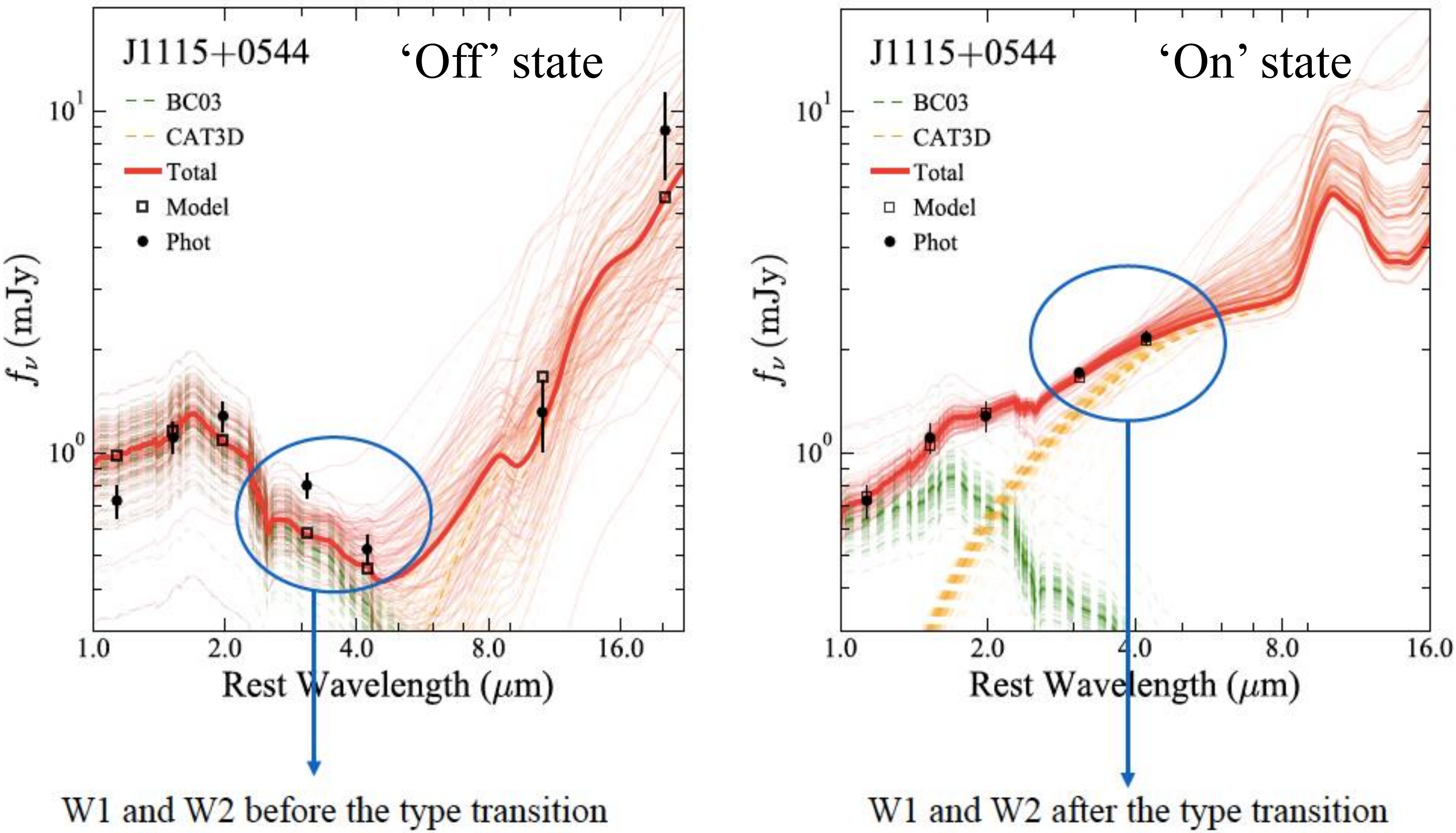

The mid-infrared W1-W2 color is redder when brighter. This is possibly due to a stronger contribution to W2 than W1 from the AGN dust torus when AGN turns on.

More to come…

(Yang et al. 2019, in prep.)

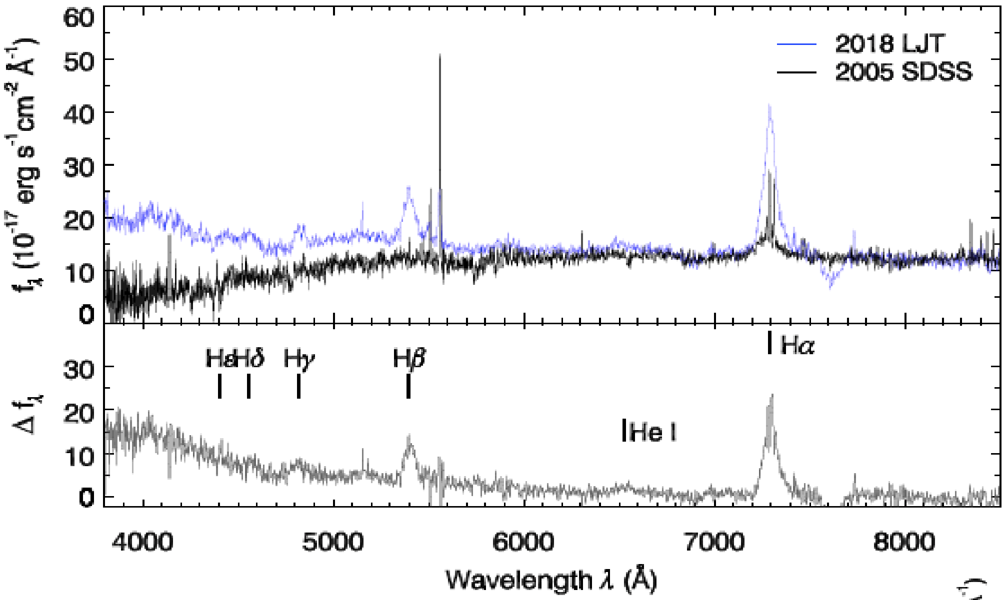

J1111

J1012

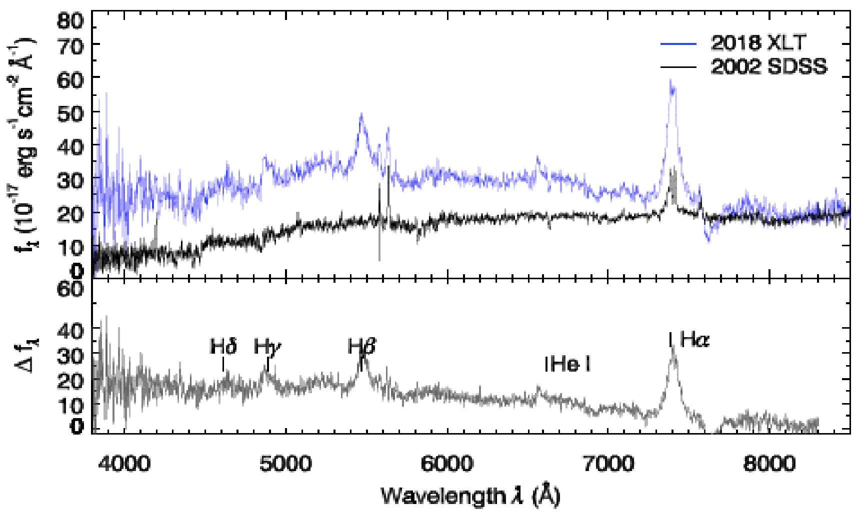

An unusual MIR flare in a Type II AGN

(Yang, Shen, Liu, Wu, et al. 2019, arXiv:1907.12721)

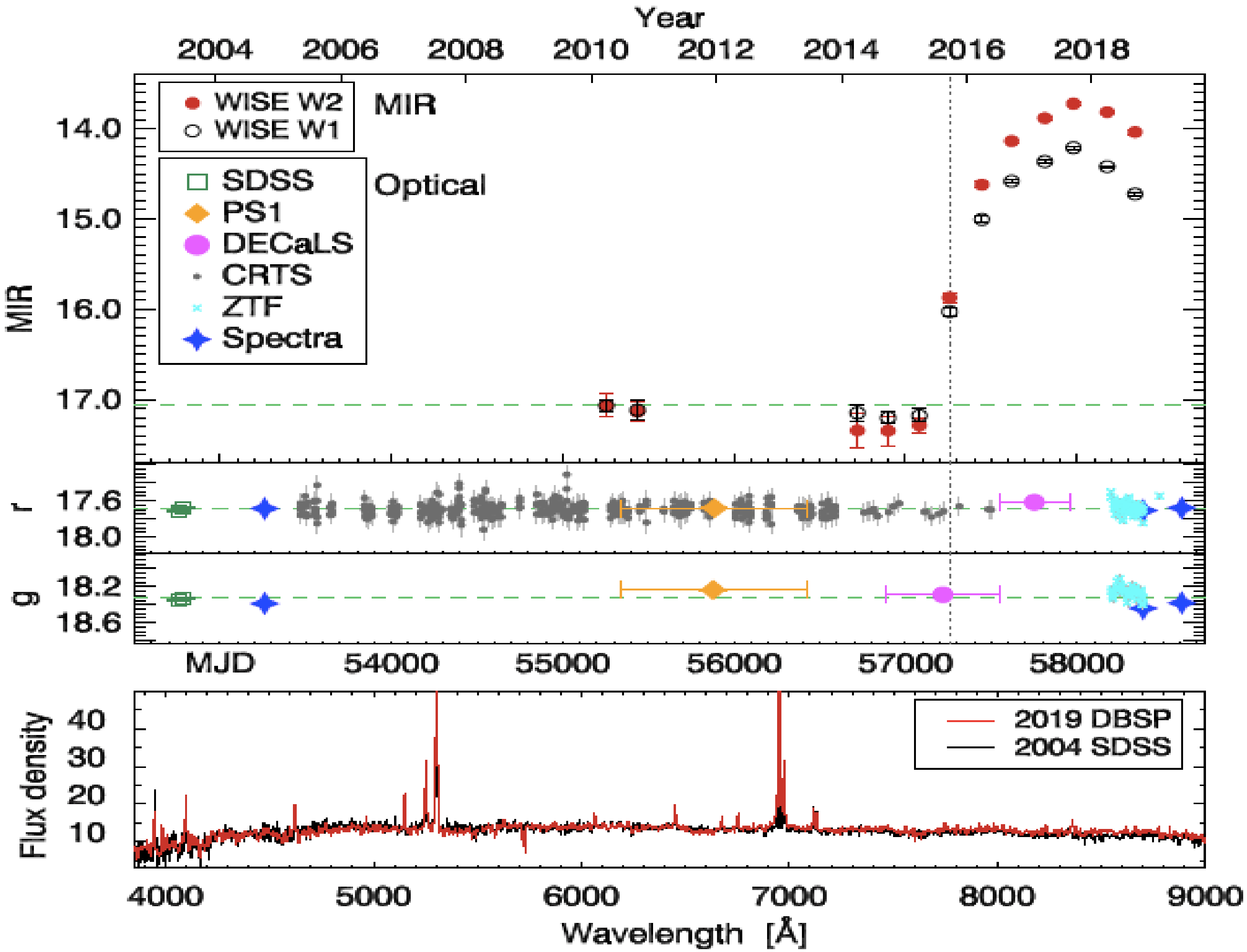

CL AGN or TDE?

Without optical variation

Figure 1. Top panel: Light curves of J1657+2345 in MIR from *WISE* and in optical from various surveys, including SDSS, PS1, DECaLS, CRTS, and ZTF. All magnitudes are AB magnitudes. To compare the optical and MIR data, the y-axis in the

3. Challenges to theoretical models

- CL AGNs challenge both the AGN unification scheme and the long-term evolution scenario between Type 1 and Type 2 AGNs
- Three models currently under debate:

No – Variable obscuration due to the movement of obscuring material (e.g., Nenkova et al. 2008a,b; Elitzur 2012)

No – A tidal disruption event (TDE) of a star disrupted by the supermassive black hole (SMBH), which may also result in a change of classification (Eracleous et al. 1995; Merloni et al. 2015; Blanchard et al. 2017)

Yes? – Variable accretion rate, in an evolutionary paradigm that AGN follows an evolutionary sequence from Type 1 to intermediate type and later to Type 2, or vice versa (e.g., Penston & Perez 1984; Elitzur et al. 2014)

Rapid change of accretion rate in CLQs?

- Viscous timescale (in years) in standard thin-disk model (Shakura & Sunyaev 1973; Eq. (5) in LaMassa et al. 2015 for SDSS J0159+0033)

$$t_{\rm infl} = 31 \left[\frac{\alpha}{0.1}\right]^{-1} \left[\frac{\lambda_{\rm Edd}}{0.03}\right]^{-2} \left[\frac{\eta}{0.1}\right]^{2} \left[\frac{r}{10\, r_{\rm g}}\right]^{7/2} \left[\frac{M_8}{1.7}\right],$$

- Unless the change occurs in the immediate vicinity around the black hole, it is usually too long for CL AGNs (more than 10,000yrs for $r \sim 100 r_g$)

Timescales in accretion disks

- Orbit: $t_{\text{orb}} \sim 1/\Omega$, where $\Omega = \sqrt{GM_{\text{BH}}/R^3}$
- Thermal: $t_{\text{th}} \sim t_{\text{orb}}/\alpha$
- Front: $t_{\text{front}} \sim (h/R)^{-1} t_{\text{th}}$
- Viscous: $t_{\nu} = (h/R)^{-2} t_{\text{th}}$

Stern et al., 2018, ApJ

$$t_{\text{orb}} \sim 10 \text{ days} \left(\frac{M_{\text{BH}}}{10^8 M_{\odot}}\right)\left(\frac{R}{150 r_g}\right)^{3/2}$$

$$t_{\text{th}} \sim 1 \text{ year} \left(\frac{\alpha}{0.03}\right)^{-1}\left(\frac{M_{\text{BH}}}{10^8 M_{\odot}}\right)\left(\frac{R}{150 r_g}\right)^{3/2}$$

$$t_{\text{front}} \sim 20 \text{ years} \left(\frac{h/R}{0.05}\right)^{-1}\left(\frac{\alpha}{0.03}\right)^{-1}\left(\frac{M_{\text{BH}}}{10^8 M_{\odot}}\right)\left(\frac{R}{150 r_g}\right)^{3/2}$$

$$t_{\nu} \sim 400 \text{ years} \left(\frac{h/R}{0.05}\right)^{-2}\left(\frac{\alpha}{0.03}\right)^{-1}\left(\frac{M_{\text{BH}}}{10^8 M_{\odot}}\right)\left(\frac{R}{150 r_g}\right)^{3/2}.$$

4. Summary

- Spectral state transitions are common in BH X-ray binaries, which can be explained by accretion rate/mode changes. Changing-look AGNs are rare, and challenge the AGN unification scheme and theoretical models
- Using repeat spectra from SDSS and LAMOST, as well as new spectra of candidates selected from optical/mid-IR photometric variability, we discovered 21 new CLQs in northern sky, leading to a large key sample to study the BH - host galaxy co-evolution
- Rapid change of accretion rate with time scales of years in the innermost part of accretion disks is preferred for CL AGNs, but further study is still needed for a coherent understanding of the changing-look BH systems at different scales.